Journal of Energy Chemistry 26 (2017) 593–601

Contents lists available at ScienceDirect

Journal of Energy Chemistry

journal homepage: www.elsevier.com/locate/jechem

http://www.journals.elsevier.com/journal-of-energy-chemistry/

Review

Electrochemical reduction of CO_2 in solid oxide electrolysis cells

Lixiao Zhang[a,b], Shiqing Hu[a,b], Xuefeng Zhu[a,*], Weishen Yang[a,*]

[a] State Key Laboratory of Catalysis, Dalian Institute of Chemical Physics, Chinese Academy of Sciences, Dalian 116023, Liaoning, China
[b] University of Chinese Academy of Sciences, Beijing 100049, China

ARTICLE INFO

Article history:
Received 9 March 2017
Revised 3 April 2017
Accepted 5 April 2017
Available online 22 April 2017

Keywords:
CO_2 electrochemical reduction
SOECs
Ni–YSZ
MIECs

ABSTRACT

The effort on electrochemical reduction of CO_2 to useful chemicals using the renewable energy to drive the process is growing fast recently. In this review, we introduce the recent progresses on the electrochemical reduction of CO_2 in solid oxide electrolysis cells (SOECs). At high temperature, only CO is produced with high current densities and Faradic efficiency while the reactor is complicated and a better sealing technique is urgently needed. The typical electrolytes such as zirconia-based oxides, ceria-based oxides and lanthanum gallates-based oxides, anodes and cathodes are introduced in this review, and the cathode materials, such as conventional metal–ceramics (cermets), mixed ionic and electronic conductors (MIECs) are discussed in detail. In the future, to gain more value-added products, the electrolyte, cathode and anode materials should be developed to allow SOECs to be operated at temperature range of 573–873 K. At those temperatures, SOECs may combine the advantages of the low temperature system and the high temperature system to produce various products with high current densities.

Lixiao Zhang is currently studying for a PhD degree from Dalian Institute of Chemical Physics at University of Chinese Academy of Sciences, China. She received her BS degree in Chemistry from Zhengzhou University in 2014. Her research interest is the electrochemical reduction of CO_2 in solid oxide electrolysis cells (SOECs).

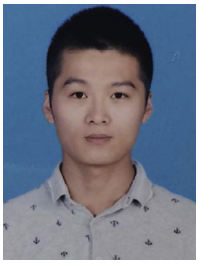

Shiqing Hu is currently studying for an MS degree from Dalian Institute of Chemical Physics at University of Chinese Academy of Sciences, China. He received his BS degree in Chemistry from Yunnan University in 2015. His research interests is the conversion and utilization of CO_2, especially for the research of high temperature co-electrolysis of CO_2–H_2O to produce sustainable fuels in solid oxide electrolytic cells (SOECs).

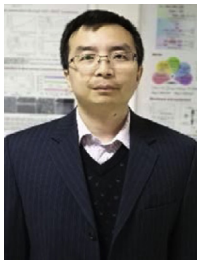

Xuefeng Zhu is a professor of Dalian Institute of Chemical Physics (DICP), Chinese Academy of Science (CAS). He received his PhD degree from CAS in 2007, and became a full professor at DICP in 2014. He has coauthored more than 70 peer-reviewed scientific papers, published one book, contributed two chapters and holds 11 patents. His research interests focus on ceramic membranes, solid state oxide cells and electrocatalysis for energy conversion.

Weishen Yang is Chair Professor of Dalian Institute of Chemical Physics, Chinese Academy of Sciences (CAS), China. He received his PhD from CAS in 1990. As a visiting scholar, he worked in Birmingham University (UK) in 1989, and University of Southern California (USA) in 2001. He works on the rational design and molecular-level engineering of functional nano-materials for applications in catalysis, and separation (e.g., inorganic membranes).

* Corresponding authors.
E-mail addresses: zhuxf@dicp.ac.cn (X. Zhu), yangws@dicp.ac.cn (W. Yang).

http://dx.doi.org/10.1016/j.jechem.2017.04.004

1. Introduction

Nowadays, the energy consumption is continuously increasing with the fast development of the global economy and the rapid increase of the emission of pollutants. Meanwhile, the main energy sources are fossil fuels, such as coal, petroleum and natural gas, since the industrial revolution in the 19th century [1]. These fossil fuels are non-renewable with limited reserves in the earth. With the combustion of fossil fuels, a large amount of green-house gas, CO_2, is released to the atmosphere, which causes climate changes, a rise in sea level, glacier ablation and so on. Therefore, alleviating the green-house effect is a pressing issue in the modern society [2].

To solve this problem, new processes related to the reduction of CO_2 and conversion of CO_2 into useful materials will be gradually attractive in the near future. In the past several years, fossil fuels have been partially replaced by the other clean and renewable energy sources, such as wind, tide, solar energy, to reduce CO_2 emission. However, these renewable energies cannot continuously produce electric power, and cannot be merged into electric net directly. Carbon capture and sequestrations (CCS) was proposed to reduce CO_2 emission [3]. Unfortunately, the CCS technology is expensive, consumes a lot of energy, and faces the risk of the stored-CO_2 leaking. Hence, the technologies related to the conversion of CO_2 into value-added chemicals have gained more and more attentions from governments and academic circles. There are three types of process to convert CO_2 into valued-added chemicals, i.e. thermal-catalysis process, photo-catalysis process and electrochemical process [4].

Recently, the electrochemical reduction of CO_2 has attracted more attentions of researchers due to many advantages. For example, the electrochemical reduction process is controllable through adjusting electrode potentials and reaction temperature. It is smart to use the electric power produced by the clean and renewable energies to drive the electrochemical reduction process. In other words, the electrochemical reduction of CO_2 can combine the development of clean and renewable energies and the utilization of CO_2 to produce value-added chemicals at mild conditions. Hence, the electrochemical reduction of CO_2 is a promising pathway to reduce CO_2 emission [5–7].

In this review, the progresses related to the electrochemical reduction of CO_2 at high temperatures in the solid oxide electrolysis cells (SOECs) are introduced in detail. A SOEC has three components: an electrolyte for the transport of the ions and preventing the crossover of the gas at the electrodes, an anode for the oxidation reaction and a cathode for the reduction reaction [9–11].

2. The electrochemical reduction of CO_2 in solid oxide electrolysis cells

The electrochemical reduction of CO_2 can pass through various pathways, i.e. two-, four-, six-, eight-, and twelve-electrons reduction [12,13]. Thus, it corresponds to various products, including carbon monoxide (CO), formic acid (HCOOH) or formate ($HCOO^-$), oxalic acid ($H_2C_2O_4$) or oxalate ($C_2O_4^{2-}$), formaldehyde (CH_2O), methanol (CH_3OH), methane (CH_4), ethylene (CH_2CH_2), ethanol (CH_3CH_2OH) and so on [14]. One is the electrochemical reduction in solutions at low temperature (<373 K), and the other is in the SOECs at high temperature (>873 K). For the electrochemical reduction operated in aqueous solutions [5,8,12], the electrolytes are usually $KHCO_3$, $NaHCO_3$ etc.; the electrochemical reactors are simple and easily fabricated; and the products are various, such as CO, HCOOH, HCOH, C_2H_5OH, C_2H_4. However, the current densities are very low due to the limitation of the mass transport of CO_2 to the cathode surface. The designs of the gas-diffusion-electrode and the optimized fabrication of the electrochemical reactors may solve this problem. The possibility of hydrogen evolution reaction in aqueous solution may decrease Faradic efficiency (FE) of the desired products. Therefore, the catalysts for electrochemical reduction of CO_2 should have high hydrogen evolution overpotentials. Ionic liquids may be another approach for the electrochemical reduction of CO_2. Compared with aqueous electrolytes, they have higher CO_2 solubility and wider potential windows, which lead to the electrochemical reduction of CO_2 much easier and the hydrogen evolution more difficult. In addition, exploring new electrocatalysts to highly selective production of target chemicals is still important in the future.

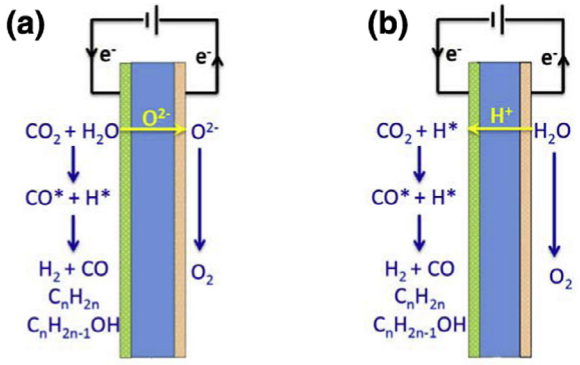

Fig. 1. The electrochemical reduction of CO_2 based on (a) the oxygen ionic conductors and (b) the protonic conductors.

Although the electrochemical reduction of CO_2 at low temperature (<373 K) can produce various products, the current density is limited by the slow mass transport and slow diffusion kinetics, since CO_2 has low solubility in aqueous electrolytes. Therefore, the electrolysis of CO_2 in a solid oxide cell at high temperatures (higher than 873 K) has gained more attentions recently. A typical solid oxide electrolysis cell (SOEC) includes electrolyte for ionic transport, anode for the evolution of oxygen and cathode for the electrochemical reduction of CO_2. Typically, the solid electrolytes can be classified into two types, i.e. oxygen ionic conductors and protonic conductors. In a solid oxide electrolysis cell using oxygen-ion-conducting electrolytes, CO_2 and H_2O molecules at the cathode receive electrons and decompose to form oxygen ions, then the oxygen ions pass through the electrolyte membrane to arrive the anode; at the anode the oxygen ions lose electrons and are oxidized to oxygen gas. At the same time, the reduced adsorbed-carbon species can react with the activated-hydrogen species to produce value-added chemicals, as shown in Fig. 1(a). While for a solid oxide electrolysis cell using protonic electrolyte, the H_2O molecule at the anode is oxidized to oxygen gas accompanied with the production of protons. Then, the protons pass through the electrolyte membrane to arrive the cathode where they react with the adsorbed-CO_2 to produce the value-added chemicals, as shown in Fig. 1(b). In a SOEC, the reactions on both anode and cathode take place at the triple phase boundaries (TPB) which comprise oxygen ionic conductors or protonic conductors, electronic conductors and the reactant gases. Therefore, the mass transport of CO_2 is not the limiting step for the electrochemical reduction of CO_2. In other words, the current density of SOECs is much higher than that of electrochemical reduction of CO_2 in aqueous electrolytes. Additionally, at high temperatures, the activation of CO_2 becomes easy, which also results in high current density. However, only CO is the main carbon-containing products, while C and methane are the by-products. The SOECs are ceramic devices involved with complicated catalytic chemistry and ceramic techniques [15]. In the following, the progresses on the components of the SOECs are separately introduced.

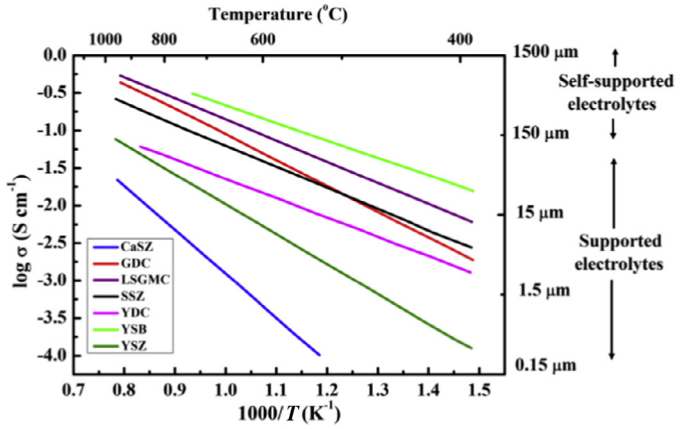

Fig. 2. Conductivity as a function of reciprocal temperature for different electrolyte materials. Reprinted from Ref. [22] with permission of the Royal Society of Chemistry.

2.1. Electrolytes

In SOECs, the electrolyte should have high oxygen ionic or protonic conductivity and negligible electronic conductivity [16,17]. Also, the electrolyte should be stable under variable redox conditions and CO_2/steam atmosphere. Meanwhile, the electrolyte should be easily shaped into dense, thin, strong film to prevent the mixture of the gases at the anode and cathode sides [18]. Researchers have made hard efforts to develop oxygen ions and protons conducting materials, and now there are many types of materials available as the electrolytes of SOECs, such as zirconia-based oxides, ceria-based oxides, lanthanum gallates-based oxides [19], bismuth-based oxides [20], barium cerate perovskite oxides etc. Fig. 2 shows the conductivities of some common electrolytes at different temperatures. In order to gain the high conductivities, the operation should be at a high temperature (>873 K) [21].

Zirconia-based oxides, such as yttria-stabilized-zirconia (YSZ, Y_2O_3 is usually 8 mol%) is the most common electrolyte material because of its high ionic conductivity, low electronic conductivity, high stability and mechanical strength, low cost and easy availability. The ionic conductivity of YSZ (8 mol% Y_2O_3) is 0.1 S/cm at 1273 K while 0.03 S/cm at 1073 K [23]. In addition, Sc_2O_3 stabilized ZrO_2 (ScSZ) shows much higher ionic conductivity than YSZ [24]. For example, 10ScSZ (Sc_2O_3 is 10 mol%) is 0.12 S/cm at 1073 K, and 8ScSZ (Sc_2O_3 is 8 mol%) is 0.24 S/cm at 1273 K; however, that of 8ScSZ decreases to 0.13 S/cm after annealing for 2000 h at 1273 K. In order to improve the stability of ScSZ, the incorporation of other cations in zirconia has been reported. For example, ZrO_2 co-doped with Sc_2O_3 and CeO_2 showed much higher ionic conductivity than YSZ during 573 K–1373 K and better long-term stability than ScSZ. Thus, $Sc_{0.1}Ce_{0.01}Zr_{0.89}O_{1.95}$ is a promising material as the electrolyte of intermediate temperature SOECs. However, because of the high cost of the scandium element and the phase change induced degradation of ScSZ at high temperature, YSZ is still the most extensively used oxygen ionic conductor. However, the low ionic conductivity of YSZ limits its application at low temperatures (<673 K) [23,25,26].

Ceria-based oxides have higher ionic conductivity than YSZ at intermediate-low temperatures and lower cost than lanthanum gallates-based perovskite oxides [27]. The most challenges of ceria-based oxides are the reduction of Ce^{4+} to Ce^{3+} under low oxygen partial pressure or high temperature or high applied voltages. This conversion causes two main problems. (1) It produces n-type electronic conduction and results in a partial internal electronic short circuit in the cell. (2) The conversion generates a notable chemical expansion of the lattice, thus leads to the mechanical fail of the electrolyte membrane. Furthermore, during the shift from the SOFCs mode to the SOECs mode [28], the applied voltage sharpens the maximum tensile stress by seven times and raises the minimum permitted oxygen partial pressure at the cathode–electrolyte interface. It was reported that the ceria-based oxides electrolytes have a trend of collapse at 973 K even 873 K under SOEC mode. Therefore, the ceria-based oxides are limited as the solid electrolyte of SOECs. However, it was reported that $Ce_{0.90}Gd_{0.10}O_{2-\delta}$ (GDC10) is stable at reduced oxygen pressures below 1000 K. Adding small amounts of praseodymium oxide into $Ce_{0.80}Gd_{0.20}O_{2-\delta}$ (GDC20) leads to better stability of GDC20 but for GDC10 is insignificant. However, Pr-doped CeO_2 has some electronic conduction under a reducing atmosphere, which decreases the performance of SOEC [29]. In addition, ceria-based composites, such as 20SDC-Li_2CO_3–Na_2CO_3, were reported as the electrolytes. They show both high protonic and oxygen ionic conductivity and low electronic conductivity, but they are not all-ceramics [16].

Lanthanum gallates-based perovskite oxides (ABO_3) doped by Sr in La (A) sites and Mg in Ga (B) sites respectively, forming $La_{1-x}Sr_xGa_{1-y}Mg_yO_{3-\delta}$ (LSGM), show high oxygen ionic conductivity [30]. For example, the oxygen ionic conductivity of $La_{0.9}Sr_{0.1}Ga_{0.8}Mg_{0.2}$ is 0.15 S/cm at 1073 K, which is comparable to that of ceria-based oxygen ionic conductors and significantly exceeds that of YSZ. The oxygen ionic conductivity of LSGM has a tendency to increase with the increase of A/B cation substitution. Under oxidizing atmosphere, the conductivity is almost ionic conductivity while a slight electronic conductivity is observed under reducing atmosphere, which is due to the reduction of Ga^{3+} to Ga^{2+}. The electronic conductivity is negligible compared with its ionic conductivity, and thus has little impact on the performance of SOECs and SOFCs. However, LSGM easily reacts with NiO to form $LaNiO_3$ phase, which causes the instability of lanthanum gallate-based electrolytes, significant increase of the electronic conductivity and the increase of electrode overpotential [31]. In order to block the interdiffusion of La and Ni components between the electrolyte and the electrode layers, various barrier interlayers are employed, such as ScSZ, GDC, La_2O_3-doped ceria. Moreover, the mechanical strength of LSGM is poor, so its application is very limited [32,33].

The proton conducting electrolytes are oxides with perovskite-related structure, such as Ba (Zr, Ce)O_3. $BaCeO_3$ is not stable in H_2O and CO_2 atmosphere, while $BaZrO_3$ has poor sintering activity and high grain-boundary resistance [34]. Nowadays, Zr, Y and Yb co-doped $BaCeO_3$ are suggested as the electrolyte of SOFCs, but few studies using it as the electrolyte of SOECs for CO_2 electrochemical reduction. The most likely reason is the low structural stability of $BaCe_{1-x-y-z}Zr_xY_yYb_zO_{3-\delta}$ under an atmosphere containing high concentrated CO_2 and steam [21].

2.2. Cathodes

The cathodes should have high ionic and electronic conductivity, good stability under an atmosphere containing high concentrated CO_2 and steam at high temperatures, excellent catalytic activity, proper porosity and good compatibility with electrolyte materials. The typical cathodes are the metal–ceramics (cermet) such as Ni–YSZ, in which Ni provides the electronic transport path and YSZ (electrolyte material) provides the ionic diffusion path.

2.2.1. The conventional metal–ceramic cathodes

Similar to that occurring on SOFCs electrode, electrolysis reactions only happen at triple phase boundaries (TPB) where Ni particles (electronic conducting phase), YSZ particles (ionic conducting phase) and gas phase meet together. Therefore, the cell performance may be limited by the available reaction sites or the length of TPB. Except TPB, other factors also have important influences

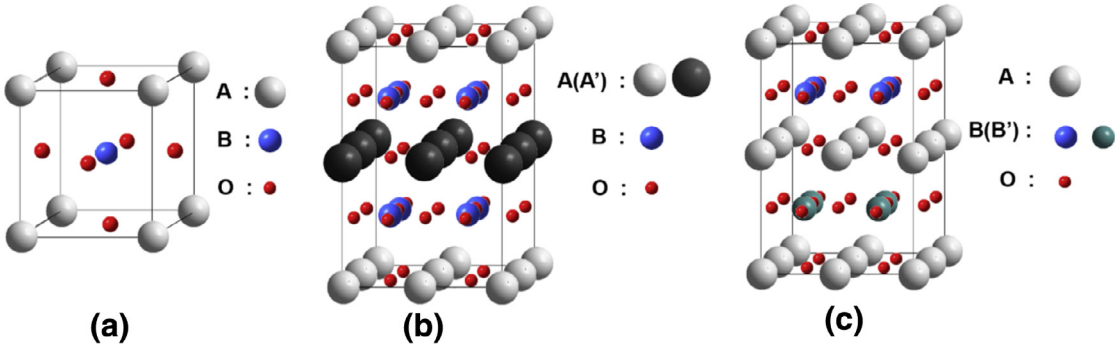

Fig. 3. The crystal structures of (a) perovskite oxides (ABO_3), (b) A-site ordered double perovskite oxides ($AA'B_2O_{5+\delta}$), and (c) B-site ordered double perovskite oxides ($A_2BB'O_{6-\delta}$).

on the performance of SOECs for CO_2 electrochemical reduction. Ebbesen and co-workers observed increased polarization in a SOEC when they decreased the porosity of the Ni–YSZ cathode structure, which indicated that diffusion limitations cannot be neglected for the cathode with porosity below 30% (with a support thickness of 300 μm). These diffusion limitations create an increased reducing atmosphere at the interface of the support and active electrode, and lead to the degradation of the cell [35]. The surface oxidation of the nickel particles, leads to the loss of electronic conductivity and the cell degradation during H_2O electrolysis or H_2O–CO_2 co-electrolysis operation at high temperatures [36]. In addition, coke deposition forms easily on Ni particles under the high temperature CO_2 electrolysis. For example, Tao et al. reported carbon formation in SOECs with a low porosity of Ni–YSZ cathode during the co-electrolysis of H_2O and CO_2 when the cells were operated at current densities of 2.0–2.25 A/cm^2 with a reactant (H_2O+CO_2) conversion of 67%. However, for cells with a higher porosity, no carbon formed [37]. Knibbe et al. found that a consequence of absorbed impurities in the Ni–YSZ hydrogen electrode can cause the cell degradation [38]. Additionally, it was reported that zirconia nanoparticles would form on the surface of Ni and at the interface of Ni–YSZ that causes the increase of the ohmic resistance and O^{2-} transport resistance [39].

Therefore, many efforts have been made to replace the Ni–YSZ cathode. For example, Cheng et al. reported the reduction of CO_2 to CO on a Cu-ceria-gadolinia cathode. The configuration of the cell is Cu/GDC|YSZ|YSZ/LSM|LSM. They observed that the Cu/GDC cathode has a comparable performance with Ni/YSZ cathode for CO_2 reduction at 1023 K with a feed of 50 vol% CO_2–50 vol% CO [40]. No significant Cu sintering/migration, carbon deposition or electrode delamination were observed during 2 h operation at 1.85 V and 1023 K. Lee et al. showed a higher hydrogen production rate (1.8 cm^3/min) on a Cu/YSZ (volume ratio of 60:40) cathode than that (1.4 cm^3/min) on the Ni/YSZ cathode (volume ratio of 60:40). However, taking the catalytic activity and the stability into the consideration, Ni–YSZ is still a potential cathode for SOECs [41].

2.2.2. Mixed ionic and electronic conductors (MIECs)

Although the conventional metal–ceramic materials (particularly, Ni/YSZ cermet) are widely used as the cathode in SOECs because of their highly electrocatalytic activity and excellent conductivities, they still suffer from reversible or irreversible performance degradation induced by metal particles oxidation, carbon deposition, grain coarsening, impurities contamination etc. [42–47]. Therefore, the conventional metal–ceramic cathode cannot be applied in practice until these problems are well solved in future. To overcome these drawbacks which also exist in SOFCs, novel materials are continuously developed as candidates for the fuel electrodes. MIECs perovskite-type oxides, whose structures are shown in Fig. 3, have been proven to be the most promising replacement to the conventional Ni/YSZ cermet in SOECs [48–50]. They demonstrate good coking resistance, high sulfur tolerance, high redox stability and acceptable catalytic activity. Their intrinsic conducting characteristics allow the transport of oxygen ions and electrons at the same time. Therefore, MIECs oxides expand the reactive sites to the MIECs oxides/fuel gas dual phase boundaries (DPB) rather than metal particles/YSZ/fuel gas triple phase boundaries (TPB) in the Ni/YSZ cermet, as shown in Fig. 4. As a result, the reaction rate of CO_2 should be increased with the increase in the number of reactive sites. Therefore, MIECs are reasonably considered as promising alternative materials for the cathode in SOECs. Besides the advantages of MIECs mentioned above, the oxygen vacancies existing on the surface of perovskite oxides could serve as accommodation sites for CO_2 adsorption and activation during the electrochemical reduction of CO_2 [51,52].

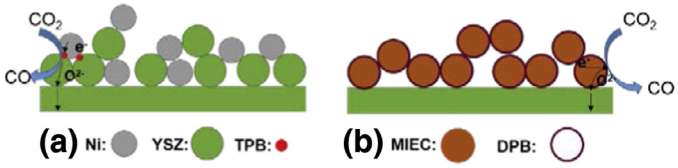

Fig. 4. Schematic diagrams of (a) TPB and (b) DPB.

Theoretically, almost all the perovskite composite oxides have the potential to be used as cathode materials in SOECs. However, considering the chemical stability under the condition of electrochemical reduction of CO_2, only a few kinds of perovskite oxides were investigated in detail, including $La_{1-x}Sr_xCr_{1-y}Mn_yO_{3-\delta}$, $(Ln_xSr_{1-x})_yTiO_{3-\delta}$ (Ln = lanthanon), $LaFeO_{3-\delta}$, double perovskite oxides. Their applications as cathodes of SOECs are introduced as follows.

$La_{1-x}Sr_xCr_{1-y}Mn_yO_{3-\delta}$: The Cr-doped $La_{1-x}Sr_xMnO_{3-\delta}$ perovskite oxides have higher oxygen diffusivity than the most common cathode material of SOFCs, i.e. $La_{0.8}Sr_{0.2}MnO_{3-\delta}$ (LSM). $La_{0.8}Sr_{0.2}Cr_{0.5}Mn_{0.5}O_{3-\delta}$ (LSCM) has been successfully applied as the anode of SOFCs [53–55]. It exhibits good performance with low area specific resistance (ASR) and polarization resistance at 1173 K [54,56]. Therefore, researchers employed LSCM as the cathode of SOECs to electrolyze CO_2, and found this material showing quite stable stability at high temperatures and reducing atmosphere.

For example, Yue and Irvine [57] studied $(La_{0.75}Sr_{0.25})_{0.97}Cr_{0.5}Mn_{0.5}O_{3-\delta}/Gd_{0.1}Ce_{0.9}O_{1.95}$ (LSCM/GDC) as a composite cathode for an electrolysis cell with YSZ as electrolyte and $La_{0.8}Sr_{0.2}MnO_3$/Sc-stabilized zirconia as the anode to prove the feasibility of LSCM as the cathode for CO_2 electrolysis as well as H_2O–CO_2 co-electrolysis at 1173 K. When the feed gas was CO_2/CO mixture (70/30; total flow rate: 20 mL/min), the CO production rate reached above 1.2 μmol/(cm•s) at ~1.9 V with 96% FE.

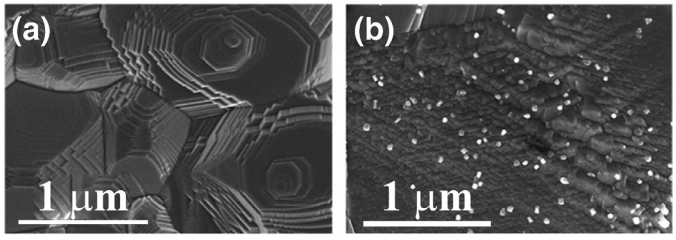

Fig. 5. SEM results of (a) oxidized LST and (b) reduced LST. Reproduced from Ref. [71] with permission from PCCP Owner Societies.

However, LSCM has a much lower electrical conductivity in reducing atmosphere, i.e. 1.5 S/cm in 5% H_2, and insufficient catalytic activity than the conventional cermet [58,59]. To solve the two problems, high electronic conducting phases are often incorporated into the LSCM electrodes. Xing et al. [60] fabricated a Cu-impregnated LSCM cathode, and found that this composite cathode displayed lower ohmic resistance and better electrochemical performances than that of the electrolysis cell without Cu impregnation from EIS and *I–V* curves under the same condition. For the electrolysis cell with Cu-impregnation cathode, the maximum current density increased from 1.31 A/cm^2 with a feed gas of 50% H_2O–50% H_2 to 1.82 A/cm^2 with a feed gas of 50% H_2O–12.5% H_2–37.5% CO_2 under the applied electrolysis voltage of 1.65 V and the temperature of 1023 K. The long-term test of the SOEC showed the applied electrolysis voltage slowly increased by 2% in 50 h under a constant current density of 0.33 A/cm^2 with a feed mixture of 50% H_2O–25% H_2–25% CO_2 at 1023 K. Besides Cu, other metals or active oxides, such as Fe, Pd, CeO_2 and V_2O_5, have been loaded on the LSCM electrode to successfully improve the electrochemical performance [61–63].

Lanthanum strontium titanates: The perovskite-type strontium titanate composites doped by La or other metal cations into A-site or B-site, are alternative materials as the cathode of SOECs [64–67]. For example, as an active and redox-stable material with high n-type electronic conductivity upon reduction, $La_xSr_{1-x}TiO_{3+\delta}$ (LST) received a great deal of interest [68,69].

The efficient electrolysis of H_2O and CO_2 has been demonstrated in an SOEC with a $La_{0.2}Sr_{0.8}TiO_{3+\delta}$ cathode by Li et al. [70]. The electrochemical results indicated that the LST cathode was stable under strongly reducing conditions and showed low electrode polarizations for the direct electrolysis of H_2O and CO_2 without reducing gases. For the electrolysis of CO_2 under ~ 2.9 V, the current density reached ~80 mA/cm^2 at 973 K with an SOEC containing a 2-mm-thick YSZ electrolyte. At the above condition, the cell offered a CO production rate of about 0.56 mL/(min•cm^2) and a low Faradic yield of 24.7%. The low Faradic yield was ascribed to the local CO_2 starvation and the low oxygen ionic conductivity of YSZ. They also investigated the surface properties and the electrocatalytic properties of the LST cathode for CO_2 electrochemical reduction, and proved that the reduced LST with n-type electronic conduction was more favorable than the unreduced LST.

To improve the performance of LST cathode for the electrochemical reduction of CO_2, Gan and co-workers [71] prepared the LST cathode by in situ growing active nickel nanoparticles socketed on the LST particles surface through manipulating the A-site non-stoichiometry of the perovskite oxide, as shown in Fig. 5. The synergetic effect of enhanced oxygen ionic conduction of the prepared LST and the catalytically active Ni nanoparticles increased the current efficiency by ~50% in contrast to the bare LST cathode for the electrolysis of CO_2. A high CO production rate (2.07 mL/(min•cm^2)) was achieved at 2.0 V with pure CO_2 as the feed gas. Further, Ye et al. [72] employed synergistic control of A-site non-stoichiometry and B-site dual doping strategy to tune LST cathode surface structures, the resulting optimized $(La_{0.2}Sr_{0.8})_{0.95}Ti_{0.85}Mn_{0.1}Ni_{0.05}O_{3+\delta}$ possessed good stability with 100 h of high-temperature operation and 10 redox cycles. The excellent performance is attributed two reasons, i.e. (1) dopant Mn promotes the formation of oxygen vacancies which could facilitate the adsorption of CO_2 and (2) dopant Ni provides metal nanoparticle exsolution promoting the catalytic activity of this cathode.

Doped lanthanum ferrites: $LaFeO_{3-\delta}$ based perovskite oxides have been intensively investigated as electrodes of both SOFCs and SOECs. These materials have shown varying levels of enhanced coking resistance, although they are accompanied by insufficient electronic conductivity and low catalytic activity [73–76].

Cao et al. [47] applied perovskite-type $La_{0.3}Sr_{0.7}Fe_{0.7}Ti_{0.3}O_{3-\delta}$ oxide as both the anode and cathode in a symmetrical SOEC for the direct electrolysis of pure CO_2 at 1073 K. The current density was 521 mA/cm^2 at 2.0 V with an FE of 72% and the polarization resistance R_p of this SOEC was 0.08 Ω•cm^2 under the above conditions, all of which show that this $La_{0.3}Sr_{0.7}Fe_{0.7}Ti_{0.3}O_{3-\delta}$ oxide is a promising material for electrolysis of CO_2. Addo et al. [75] examined the $La_{0.3}Sr_{0.7}Fe_{0.7}Cr_{0.3}O_{3-\delta}$ perovskite as a CO/CO_2 fuel electrode material for symmetrical, reversible solid oxide fuel cell applications, showing high and stable performance toward CO_2 electrolysis and oxidation of CO. The polarization resistance at 1073 K and open circuit potential in 90% CO_2–10% CO was 0.9 Ω•cm^2, while a degradation rate of only 0.057 mV/h was observed after ~135 h of galvanostatic testing at 100 mA/cm^2 in 90% CO_2–10% CO at 1073 K. This group also researched its electrochemistry properties under different conditions e.g. air, pure CO_2 and a 1:1 CO_2:CO over a temperature range of 923–1073 K. They found $La_{0.3}Sr_{0.7}Fe_{0.7}Cr_{0.3}O_{3-\delta}$ was active in all above environments, but oxygen evolution is somewhat more facile than oxygen reduction, and CO_2 reduction is more active than CO oxidation on the $La_{0.3}Sr_{0.7}Fe_{0.7}Cr_{0.3}O_{3-\delta}$ electrodes [76].

It is noteworthy that Liu et al. [77] developed a novel cathode prepared by reducing the Sr and Ni co-doped $LaFeO_3$ perovskite oxide, i.e. $La_{0.6}Sr_{0.4}Fe_{0.8}Ni_{0.2}O_{3-\delta}$ (LSFN), in H_2 atmosphere at 1123 K. The Fe–Ni bimetallic alloy nanoparticles were successfully exsolved in situ and uniformly socketed on the oxygen deficient perovskite backbone. The cathode kinetics for CO_2 electrolysis was significantly improved with a remarkably enhanced current density of 1.78 A/cm^2 and together with a high FE of 98.8% at 1.6 V and 1123 K. No obvious degradation and discernible carbon deposition were observed on this cathode after operating for over 100 h. For a similar purpose, another method was employed to improve the performance of lanthanum ferrites-based cathode. Zhang et al. [52] introduced the catalytic and redox active Ce into A-site of $La_{0.7}Sr_{0.3}Cr_{0.5}Fe_{0.5}O_{3-\delta}$ (Ce-LSCrF) to promote the catalytic activity and introduce more oxygen vacancies in the lattice in situ after reduction. The increased number of oxygen vacancies not only facilitates the mobility of oxygen ions, but also provides favorable accommodations for chemical adsorption of CO_2. For the CO_2 electrolysis, the FE of Ce-LSCrF based SOECs reached around 86.9% at applied voltage of ~1.56 V, notably higher than that of the undoped LSCrF sample (64.7%), and the current was slightly increased by ~0.1 A/cm^2, as shown in Fig. 6. However, there exists an optimal surface oxygen vacancy concentration in perovskite oxides that balances the oxygen exchange kinetics and the chemical stability [78].

Double perovskite oxides: Double perovskite oxides with general formula $AA'B_2O_{5+\delta}$ or $A_2BB'O_{6-\delta}$, as shown in Fig. 3(b) and (c), where A denotes rare earth, A' denotes an alkaline earth, B and B' generally denote Ni, Co, Fe, Mo, Mn etc., have obtained a great deal of attention in recent years for their exceptional electrochemical properties, such as $PrBaMn_2O_{5+\delta}$ [79], $PrBa_{0.5}Sr_{0.5}Co_{1.5}Fe_{0.5}O_{5+\delta}$ [80], $Sr_2Mg_{1-x}Mn_xMoO_{6-\delta}$ [81], $Sr_2FeMo_{0.65}Ni_{0.35}O_{6-\delta}$ [82]. Most of them have been used as electrodes in SOFCs and achieved high performances. Researchers are attempting to apply this kind of

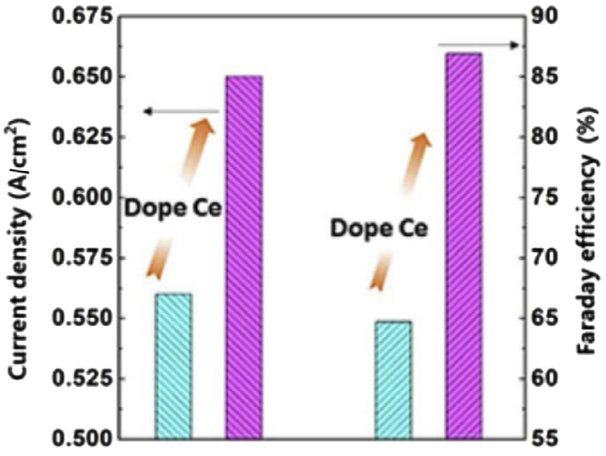

Fig. 6. Comparison of the current density and FE of the Ce-doped LSCrF and LSCrF. Reprinted with permission from Ref. [52]. Copyright © 2016, American Chemical Society.

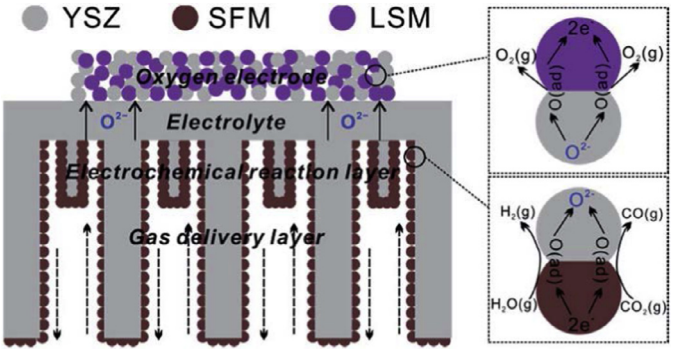

Fig. 7. Schematic diagram of the hierarchically porous YSZ cathode scaffold with infiltrated SFM. Reproduced from Ref. [84] with permission of The Royal Society of Chemistry.

materials to SOECs because of their high electronic conductivity and oxygen ionic conductivity.

Wang et al. [83] demonstrated a symmetrical SOEC with $Sr_2Fe_{1.5}Mo_{0.5}O_{6-\delta}$–$Sm_{0.2}Ce_{0.8}O_{1.9}$ composite as both the cathode and anode materials for H_2O/CO_2 co-electrolysis. The results exhibited that this SOEC has excellent electrochemical performance with the current density of 0.734 A/cm^2 at 1.3 V and the interfacial polarization resistance of 0.48 Ω•cm^2 at 1123 K. Furthermore, the electrolysis cell exhibits no coking but an increased cell voltage with the rate of 0.00013 V/h under a constant current density of 0.12 A/cm^2 at 1073 K during a 100 h-test. Li et al. [84] deposited $Sr_2Fe_{1.5}Mo_{0.5}O_{6-\delta}$ (SFM) nanoparticles, which act as the electrocatalysts, onto the inner surface of the hierarchically porous YSZ scaffold, as shown in Fig. 7. To our best of knowledge, they achieved the highest performance in all the published results up to now for pure CO_2 electrolysis with the electrode polarization resistance of 0.25 Ω•cm^2 under the current density of 1.1 A/cm^2 at 1.5 V and in the pure CO_2 of 20 mL/min. Therefore, double perovskite oxides are likely to provide an opportunity for the rapid development of SOECs.

2.3. Anodes

In high temperature SOECs, anode is the catalyst for oxygen evolution reaction (OER). The anode should have both high ionic and electronic conductivities, high catalytic activity for oxygen evolution, and good compatibility with other cell components. There are three main types of anode: perovskite oxides, double perovskite oxides and Ruddlesden–Popper (RP) oxides. And less expensive perovskite oxides are the most frequently investigated materials nowadays.

2.3.1. Perovskite anodes

$La_{1-x}Sr_xMnO_{3-\delta}$ (LSM) is the most common anode material, but its ionic conductivity is very low. Therefore, YSZ is added to form the LSM–YSZ composite anode to provide the ionic conductivity and increase the triple phase boundaries (TPB) [85,86]. For example, Xia and co-workers [87] integrated the high-temperature CO_2–H_2O co-electrolysis and low temperature Fischer–Tropsch synthesis in a single tubular unit with a LSM–YSZ anode. Meanwhile, Co and Fe-based perovskite oxides showing higher oxygen ionic conductivity than that of LSM were also considered as the anode for SOECs. Vohs et al. compared the $La_{0.8}Sr_{0.2}MnO_3$, $La_{0.8}Sr_{0.2}FeO_3$ and $La_{0.8}Sr_{0.2}CoO_3$ as the SOEC anodes. The impedances of $La_{0.8}Sr_{0.2}FeO_3$–YSZ and $La_{0.8}Sr_{0.2}CoO_3$–YSZ are essentially independent of current and are the same under anodic and cathodic polarization. However, the LSM–YSZ electrode does not appear to be optimal for OER. It showed good performance only after cathodic activation. LSM-based electrodes are easy to be fabricated. Unlike $La_{0.8}Sr_{0.2}FeO_3$–YSZ and $La_{0.8}Sr_{0.2}CoO_3$–YSZ, there is no significant solid-state reaction between LSM and YSZ below 1473 K. Eguchi et al. compared $La_{0.6}Sr_{0.4}MnO_3$ and $La_{0.6}Sr_{0.4}CoO_3$ anodes, and found LSM is more preferable than $La_{0.6}Sr_{0.4}CoO_3$ as an anode due to the small thermal expansion mismatch and poor reactivity with YSZ. The oxygen ion movements in SOECs are different from that in SOFCs. An anode delamination phenomenon has been observed in the SOEC mode while not found in the SOFC mode [88–91]. The ionic conductivity is much low, thus the oxygen evolution from the LSM electrode only occurs at the limited TPB.

To improve the performance of the LSM anode, Xie and co-workers [92] reported a composite manganite anode enhanced by iron oxide nanocatalysts for high temperature steam electrolysis in a proton conducting solid oxide electrolyzer. The size of the Fe_2O_3 nanoparticles is approximately 20–40 nm on the surface of the LSM composite anode. They investigated the LSM composite electrodes loaded with different contents of Fe_2O_3 in symmetric cells, and found the electrode loaded with 4 wt% Fe_2O_3 nanoparticles showed the most excellent performance. The maximum FE is approximately 65% for the 4 wt% Fe_2O_3-loaded LSM composite electrode while the efficiency of the LSM composite electrode without Fe_2O_3-loaded is as low as 15%, as shown in Fig. 8(a) and (b). A short-term test (10 h) based on the 4 wt% Fe_2O_3–LSM electrode for steam electrolysis was performed at 1.4 V and 1073 K, as shown in Fig. 8(c). In their another article [93], they fabricated a composite anode of Co_3O_4-loaded $La_{0.8}Sr_{0.2}MnO_3$-$BaCe_{0.5}Zr_{0.3}Y_{0.16}Zn_{0.04}O_{3-\delta}$ (BCZYZ), and found loading Co_3O_4 in the composite electrode can significantly enhance the electrode performance and the current efficiency, reaching approximately 46% for the steam electrolysis.

In addition, some researchers studied the bilayer electrode to prevent the reactivity between the anode and the electrolyte. For example, Choi and co-workers [90] inserted a GDC interlayer between YSZ electrolyte and $La_{0.6}Sr_{0.4}Co_{0.2}Fe_{0.8}O_{3-\delta}$ (LSCF) anode to improve the stability of the electrode. They found that the cell co-fired at 1673 K is the most stable cell because of the optimized reaction of the GDC interlayer with YSZ. The GDC interlayer reduces the delamination problem of LSCF and lowers ohmic and electrode polarization resistance compared with the cell without the interlayer.

2.3.2. Double perovskite anodes

A few efforts have been made to fabricate ordered double perovskite oxides as anodes of SOFCs, such as $GdBaCo_2O_{5+\delta}$,

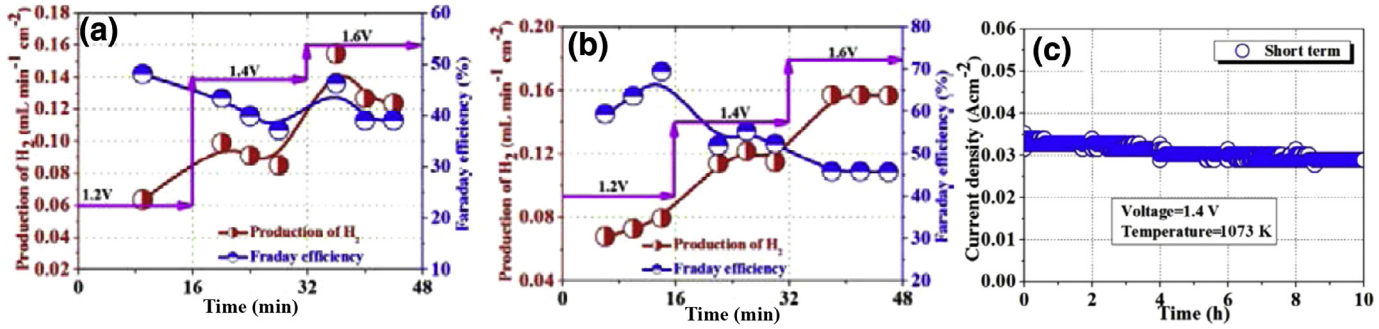

Fig. 8. H_2 production and Faradaic current efficiencies for the cells based on (a) LSM and (b) 4 wt% Fe_2O_3–LSM anode, respectively; (c) Short-term performances of the electrolysis cells based on 4 wt% Fe_2O_3–LSM anode for steam electrolysis at 1073 K. Reprinted from Ref. [92] with permission from Elsevier.

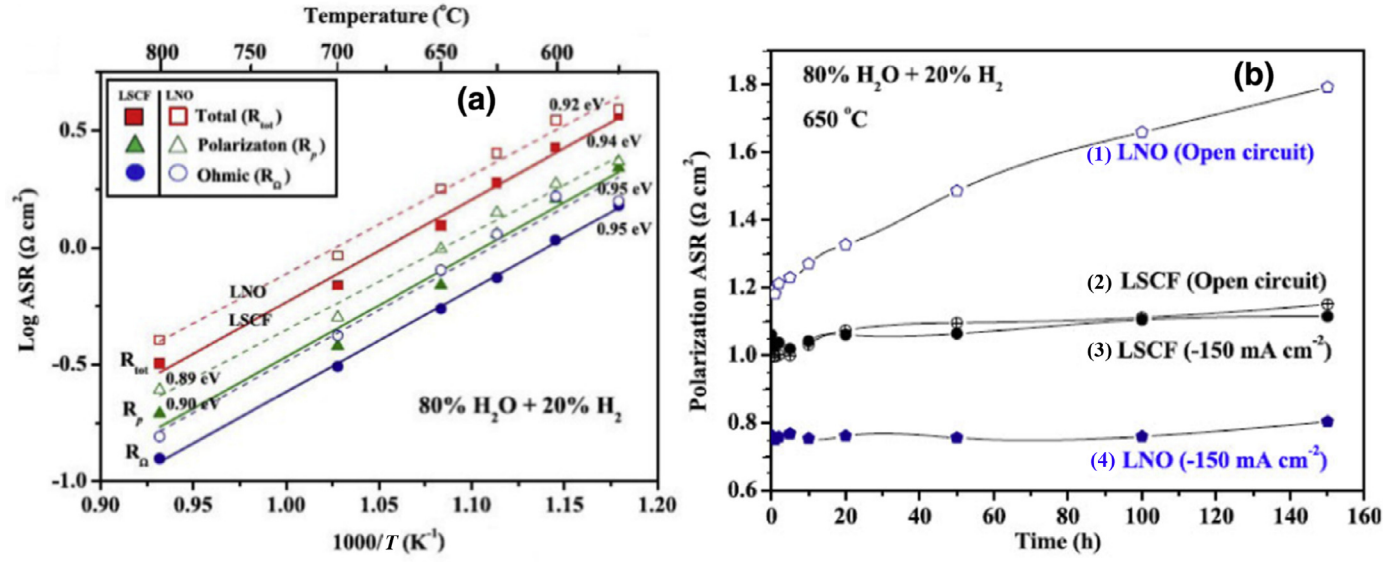

Fig. 9. (a) Total resistance, electrode polarization resistance, the ohmic resistance of LNO (open symbols) and LSCF (solid symbols) at 848–1073 K; (b) Polarization resistance as function of operation time. Reprinted from Ref. [97] with permission from Elsevier.

$PrBaCo_2O_{5+\delta}$, $Sr_2Fe_{1.5}Mo_{0.5}O_{6-\delta}$ (SFM), Nb-doped SFMO. The electrical conductivity of SFM is as high as 32 S/cm at 1073 K in hydrogen and 15 S/cm at 1023 K in air, respectively, due to the mixed-valence states of Mo^{5+}/Mo^{6+} and Fe^{3+}/Fe^{4+}. These double perovskite oxides have the potential to be used as both anode and cathode of SOEC [15]. Li et al. [94] used $Sr_2Fe_{1.5}Mo_{0.5}O_{6-\delta}$ (SFM)–$Zr_{0.84}Y_{0.16}O_{2-\delta}$ (YSZ) as anode for steam electrolysis. When the YSZ matrix was impregnated with 20 wt% SFM (SFM20), the current density of the SOEC reached to 327 mA/cm^2 at 1.2 V and 1023 K. A hydrogen production rate up to 11.46 NL/h was achieved for the SFM20-YSZ anode at 1023 K. Therefore, SFM is a promising material as the anode of SOECs. Chen and co-workers [95,96] used microwave-assisted combustion method to prepare $Sr_2Fe_{1.5}Mo_{0.5}O_3$ (SFM) as both anode and cathode in symmetrical SOEC. The cell polarization resistance is 0.26 Ω•cm^2 under open circuit voltage and 60% absolute humidity (AH) at 1173 K. The electrolysis current is 0.88 A/cm^2 and hydrogen production rate is 380 mL/cm^2 h at 1173 K and 1.3 V and 60% AH. The cell showed a good stability during the steam electrolysis test for 100 h.

2.3.3. *Ruddlesden–Popper series anodes*

The oxygen over stoichiometric rare earth nickelates, $Ln_2NiO_{4+\delta}$ (Ln = La, Pr, Nd), have the K_2NiF_4-type structure and belong to the Ruddlesden–Popper series anodes. These compounds show high electronic and ionic conductivities and high oxygen surface exchange rates. Also, they own a high oxygen content flexibility in a broad oxygen partial pressure range. Choi and co-workers [97] used $La_2NiO_{4+\delta}$ (LNO) as anode and compared the polarization and the stability of LNO with those of $La_{0.6}Sr_{0.4}Co_{0.2}Fe_{0.8}O_3$ (LSCF), as shown in Fig. 9. At the open circuit voltage, LSCF exhibited smaller polarization resistances from 848 to 1073 K and was more stable than LNO at 923 K during a 150 h-test. However, the LNO showed better performance and slower degradation rate than LSCF at a current density of 150 mA/cm^2. Grenier and co-workers [98] fabricated a three-electrode symmetrical half-cells using $Ln_2NiO_{4+\delta}$ (Ln = La, Pr or Nd) as the anode. They found that $Pr_2NiO_{4+\delta}$ showed the best performances, the current densities of which are ten times higher than that of the common perovskite $La_{0.6}Sr_{0.4}Co_{0.2}Fe_{0.8}O_{3-\delta}$ (LSCF) electrode. However, $Pr_2NiO_{4+\delta}$ reacts with YSZ and ceria-based electrolytes at high temperature. To solve that, Barnett and co-workers fabricated a $Pr_2NiO_{4+\delta}$-infiltrated porous $La_{0.9}Sr_{0.1}Ga_{0.8}Mg_{0.2}O_{3-\delta}$ anode. The polarization resistance was 0.11 Ω•cm^2 at 923 K with loading 14 vol% $Pr_2NiO_{4+\delta}$ and increased by ~10% at 923 K during a 500-h-test in a symmetrical electrolysis cell [99]. Grenier and co-workers used $Nd_2NiO_{4+\delta}$ as the anode, 3% yttria stabilized tetragonal zirconia as the electrolyte, 30 μm-thick porous nickel and gadolinia doped ceria cermet (Ni-GDC) as cathode. The current densities were 0.40, 0.64 and 0.87 mA/cm^2 at 1.3 V, which were 4.2, 3 and 1.7 times higher than the LSM anode at 1023 K, 1073 K and 1123 K, respectively, and corresponding to the hydrogen yields of 14%, 23% and 31%. Therefore, $Ln_2NiO_{4+\delta}$ oxides were regarded as good anodes for SOECs [100].

3. Conclusions and outlooks

In this review, the recent developments about the electrochemical reduction of carbon dioxide were briefly introduced. The electrochemical reduction of CO_2 in solid oxide electrolysis cells has high current densities [15]. But only CO is the main carbon-containing products, because the intermediate species for the production of other carbon-containing chemicals were easily desorbed from the surface of catalysts to produce CO at high temperatures. There are many problems about CO_2 electrochemical reduction in SOEC, such as metal particles oxidation, carbon deposition, grain coarsening, impurities contamination etc. inducing cells degradation and high complexity of electrochemical reactors, difficulty in the sealing at high temperature etc. decreasing the engineering feasibility of SOECs. In the future, deep understanding of the conventional cathode system, such as Ni–YSZ, should be well addressed to improve the stability, since the conventional cathode system has high engineering feasibility. Simultaneously, it is urgent to improve the catalytic performance of perovskite-related electrodes and explore new materials and microstructure for both the cathode and anode. Furthermore, electrochemical reduction of CO_2 in the temperature range of 573–873 K is worth exploring, because it may produce various products and achieve high current densities at the same time. However, there are no proper material systems for the electrodes and electrolyte at current stage, so the research activities on the electrochemical reduction of CO_2 at intermediate temperatures should be focused on exploring new materials and developing new methods to improve the performance of conventional materials in the future.

Acknowledgments

We thank the financial support from the National Natural Science Foundation of China (91545202), and the Strategic Priority Research Program of the Chinese Academy of Sciences (Grant No. XDB17020400).

References

[1] D.D. Zhu, J.L. Liu, S.Z. Qiao, Adv. Mater. 28 (2016) 3423–3452.
[2] K. Zhang, Z. Hu, J. Chen, J. Energy Chem. 22 (2013) 214–225.
[3] E. Berger, M.W. Hahn, T. Przybilla, B. Winter, E. Spiecker, A. Jentys, J.A. Lercher, J. Energy Chem. 25 (2016) 327–335.
[4] X. Su, J. Xu, B. Liang, H. Duan, B. Hou, Y. Huang, J. Energy Chem. 25 (2016) 553–565.
[5] J. Qiao, Y. Liu, F. Hong, J. Zhang, Chem. Soc. Rev. 43 (2014) 631–675.
[6] C. Oloman, H. Li, ChemSusChem 1 (2008) 385–391.
[7] J. Albo, M. Alvarez-Guerra, P. Castano, A. Irabien, Green Chem 17 (2015) 2304–2324.
[8] M. Bevilacqua, J. Filippi, H.A. Miller, F. Vizza, Energy Technol. 3 (2015) 197–210.
[9] S.D. Ebbesen, M. Mogensen, J. Power Sources 193 (2009) 349–358.
[10] O. Yamamoto, Y. Arati, Y. Takeda, N. Imanishi, Y. Mizutani, M. Kawai, Y. Nakamura, Solid State Ionics 79 (1995) 137–142.
[11] A. Atkinson, S. Barnett, R.J. Gorte, J.T.S. Irvine, A.J. McEvoy, M. Mogensen, S.C. Singhal, J. Vohs, Nat. Mater. 3 (2004) 17–27.
[12] I. Merino-Garcia, E. Alvarez-Guerra, J. Albo, A. Irabien, Chem. Eng. J. 305 (2016) 104–120.
[13] H. Zhong, K. Fujii, Y. Nakano, J. Energy Chem. 25 (2016) 517–522.
[14] M.R. Singh, E.L. Clark, A.T. Bell, Phys. Chem. Chem. Phys. 17 (2015) 18924–18936.
[15] S.Y. Gómez, D. Hotza, Renewable Sustainable Energy Rev. 61 (2016) 155–174.
[16] B. Zhu, I. Albinsson, C. Andersson, K. Borsand, M. Nilsson, B.-E. Mellander, Electrochem. Commun. 8 (2006) 495–498.
[17] R. Chiba, T. Ishii, F. Yoshimura, Solid State Ionics 91 (1996) 249–256.
[18] J.B. Goodenough, Annu. Rev. Mater. Res. 33 (2003) 91–128.
[19] T. Ishihara, J. Tabuchi, S. Ishikawa, J. Yan, M. Enoki, H. Matsumoto, Solid State Ionics 177 (2006) 1949–1953.
[20] N.M. Sammes, G.A. Tompsett, H. Näfe, F. Aldinger, J. Eur. Ceram. Soc. 19 (1999) 1801–1826.
[21] V.V. Kharton, F.M.B. Marques, A. Atkinson, Solid State Ionics 174 (2004) 135–149.
[22] D.J.L. Brett, A. Atkinson, N.P. Brandon, S.J. Skinner, Chem. Soc. Rev. 37 (2008) 1568–1578.
[23] O. Yamamoto, Y. Arachi, H. Sakai, Y. Takeda, N. Imanishi, Y. Mizutani, M. Kawai, Y. Nakamura, Ionics 4 (1998) 403–408.
[24] S.P.S. Badwal, F.T. Ciacchi, D. Milosevic, Solid State Ionics 136–137 (2000) 91–99.
[25] D.S. Lee, W.S. Kim, S.H. Choi, J. Kim, H.W. Lee, J.H. Lee, Solid State Ionics 176 (2005) 33–39.
[26] M. Mori, T. Abe, H. Itoh, O. Yamamoto, Y. Takeda, T. Kawahara, Solid State Ionics 74 (1994) 157–164.
[27] H. Inaba, H. Tagawa, Solid State Ionics 83 (1996) 1–16.
[28] S. Zhu, Y. Wang, Y. Rao, Z. Zhan, C. Xia, Int. J. Hydrogen Energy 39 (2014) 12440–12447.
[29] V.V. Kharton, F.M. Figueiredo, L. Navarro, E.N. Naumovich, A.V. Kovalevsky, A.A. Yaremchenko, A.P. Viskup, A. Carneiro, F.M.B. Marques, J.R. Frade, J. Mater. Sci. 36 (2001) 1105–1117.
[30] N.S. Chae, K.S. Park, Y.S. Yoon, I.S. Yoo, J.S. Kim, H.H. Yoon, Colloids Surf. A: Physicochem. Eng. Aspects 313–314 (2008) 154–157.
[31] M. Morales, J.J. Roa, J. Tartaj, M. Segarra, J. Eur. Ceram. Soc. 36 (2016) 1–16.
[32] J.W. Stevenson, T.R. Armstrong, L.R. Pederson, J. Li, C.A. Lewinsohn, S. Baskaran, Solid State Ionics 113–115 (1998) 571–583.
[33] T. Ishihara, N. Jirathiwathanakul, H. Zhong, Energy Environ. Sci. 3 (2010) 665–672.
[34] K. Katahira, Y. Kohchi, T. Shimura, H. Iwahara, Solid State Ionics 138 (2000) 91–98.
[35] S.D. Ebbesen, X. Sun, M.B. Mogensen, Faraday Discuss. 182 (2015) 393–422.
[36] T. Matsui, R. Kishida, J.-Y. Kim, H. Muroyama, K. Eguchi, J. Electrochem. Soc. 157 (2010) B776–B781.
[37] Y. Tao, S.D. Ebbesen, M.B. Mogensen, J. Electrochem. Soc. 161 (2014) F337–F343.
[38] R. Knibbe, M.L. Traulsen, A. Hauch, S.D. Ebbesen, M. Mogensen, J. Electrochem. Soc. 157 (2010) B1209–B1217.
[39] Y. Tao, S.D. Ebbesen, M.B. Mogensen, J. Power Sources 328 (2016) 452–462.
[40] C.-Y. Cheng, G.H. Kelsall, L. Kleiminger, J. Appl. Electrochem. 43 (2013) 1131–1144.
[41] S. Lee, J.-M. Kim, H.S. Hong, S.-K. Woo, J. Alloys Compd. 467 (2009) 614–621.
[42] W. Wang, C. Su, Y. Wu, R. Ran, Z. Shao, Chem. Rev. 113 (2013) 8104–8151.
[43] Y. Zheng, J. Wang, B. Yu, W. Zhang, J. Chen, J. Qiao, J. Zhang, Chem. Soc. Rev. 46 (2017) 1427–1463.
[44] A. Hauch, S.D. Ebbesen, S.H. Jensen, M. Mogensen, J. Mater. Chem. 18 (2008) 2331–2340.
[45] M.A. Laguna-Bercero, J. Power Sources 203 (2012) 4–16.
[46] Y. Tao, S.D. Ebbesen, M.B. Mogensen, J. Power Sources 328 (2016) 452–462.
[47] Z. Cao, B. Wei, J. Miao, Z. Wang, Z. Lü, W. Li, Y. Zhang, X. Huang, X. Zhu, Q. Feng, Y. Sui, Electrochem. Commun. 69 (2016) 80–83.
[48] Y. Li, J. Zhou, D. Dong, Y. Wang, J.Z. Jiang, H. Xiang, K. Xie, Phys. Chem. Chem. Phys. 14 (2012) 15547–15553.
[49] V. Singh, H. Muroyama, T. Matsui, S. Hashigami, T. Inagaki, K. Eguchi, J. Power Sources 293 (2015) 642–648.
[50] S.E. Yoon, S.H. Song, J. Choi, J.Y. Ahn, B.K. Kim, J.S. Park, Int. J. Hydrogen Energy 39 (2014) 5497–5504.
[51] J. Zhang, K. Xie, H. Wei, Q. Qin, W. Qi, L. Yang, C. Ruan, Y. Wu, Sci. Rep. 4:7082 (2014) 1–14.
[52] Y.Q. Zhang, J.H. Li, Y.F. Sun, B. Hua, J.L. Luo, ACS Appl. Mater. Interfaces 8 (2016) 6457–6463.
[53] M.A. Raza, I.Z. Rahman, S. Beloshapkin, J. Alloys Compd. 485 (2009) 593–597.
[54] S. Tao, J.T.S. Irvine, J. Electrochem. Soc. 151 (2004) A252–A259.
[55] J. Wan, J. Zhu, J. Goodenough, Solid State Ionics 177 (2006) 1211–1217.
[56] E. Raj, J. Kilner, J.T.S. Irvine, Solid State Ionics 177 (2006) 1747–1752.
[57] X. Yue, J.T.S. Irvine, Solid State Ionics 225 (2012) 131–135.
[58] S. Tao, J.T.S. Irvine, Nat. Mater. 2 (2003) 320–323.
[59] R. Xing, Y. Wang, S. Liu, C. Jin, J. Power Sources 208 (2012) 276–281.
[60] R. Xing, Y. Wang, Y. Zhu, S. Liu, C. Jin, J. Power Sources 274 (2015) 260–264.
[61] S. Xu, S. Chen, M. Li, K. Xie, Y. Wang, Y. Wu, J. Power Sources 239 (2013) 332–340.
[62] S.E. Yoon, J.Y. Ahn, B.K. Kim, J.S. Park, Int. J. Hydrogen Energy 40 (2015) 13558–13565.
[63] X. Zhang, L. Ye, J. Hu, J. Li, W. Jiang, C.J. Tseng, K. Xie, Electrochim. Acta 212 (2016) 32–40.
[64] O.A. Marina, N.L. Canfield, J.W. Stevenson, Solid State Ionics 149 (2002) 21–28.
[65] J. Canales-Vázquez, J.C. Ruiz-Morales, D. Marrero-López, J. Peña-Martínez, P. Núñez, P. Gómez-Romero, J. Power Sources 171 (2007) 552–557.
[66] X. Li, H. Zhao, F. Gao, N. Chen, N. Xu, Electrochem. Commun. 10 (2008) 1567–1570.
[67] A. Vincent, J.L. Luo, K.T. Chuang, A.R. Sanger, J. Power Sources 195 (2010) 769–774.
[68] G. Tsekouras, D. Neagu, J.T.S. Irvine, Energy Environ. Sci. 6 (2013) 256–266.
[69] J.H. Myung, D. Neagu, D.N. Miller, J.T.S. Irvine, Nature 537 (2016) 528–531.
[70] S. Li, Y. Li, Y. Gan, K. Xie, G. Meng, J. Power Sources 218 (2012) 244–249.
[71] L. Gan, L. Ye, S. Tao, K. Xie, Phys. Chem. Chem. Phys. 18 (2016) 3137–3143.
[72] L. Ye, M. Zhang, P. Huang, G. Guo, M. Hong, C. Li, J.T.S. Irvine, K. Xie, Nat. Commun. 8 (2017) 14785.
[73] M. Chen, S. Paulson, V. Thangadurai, V. Birss, J. Power Sources 236 (2013) 68–79.
[74] B. Molero-Sánchez, J. Prado-Gonjal, D. Ávila-Brande, M. Chen, E. Morán, V. Birss, Int. J. Hydrogen Energy 40 (2015) 1902–1910.
[75] P.K. Addo, B. Molero-Sanchez, M. Chen, S. Paulson, V. Birss, Fuel Cells 15 (2015) 689–696.

[76] B. Molero-Sanchez, P. Addo, A. Buyukaksoy, S. Paulson, V. Birss, Faraday Discuss 182 (2015) 159–175.
[77] S. Liu, Q. Liu, J.L. Luo, ACS Catal. 6 (2016) 6219–6228.
[78] N. Tsvetkov, Q. Lu, L. Sun, E.J. Crumlin, B. Yildiz, Nat. Mater. 15 (2016) 1010–1016.
[79] S. Sengodan, S. Choi, A. Jun, T.H. Shin, Y.W. Ju, H.Y. Jeong, J. Shin, J.T.S. Irvine, G. Kim, Nat. Mater. 14 (2015) 205–209.
[80] A. Jun, J. Kim, J. Shin, G. Kim, Angew. Chem., Int. Ed. Engl. 55 (2016) 12512–12515.
[81] Y.H. Huang, R.I. Dass, Z.L. Xing, J.B. Goodenough, Science 312 (2006) 254–257.
[82] Z. Du, H. Zhao, S. Yi, Q. Xia, Y. Gong, Y. Zhang, X. Cheng, Y. Li, L. Gu, K. Swierczek, ACS Nano 10 (2016) 8660–8669.
[83] Y. Wang, T. Liu, S. Fang, F. Chen, J. Power Sources 305 (2016) 240–248.
[84] Y. Li, P. Li, B. Hu, C. Xia, J. Mater. Chem. A 4 (2016) 9236–9243.
[85] A. Chroneos, B. Yildiz, A. Tarancon, D. Parfitt, J.A. Kilner, Energy Environ. Sci. 4 (2011) 2774–2789.
[86] Y. Huang, J.M. Vohs, R.J. Gorte, J. Electrochem. Soc. 152 (2005) A1347–A1353.
[87] L. Chen, F. Chen, C. Xia, Energy Environ. Sci. 7 (2014) 4018–4022.
[88] W. Wang, Y. Huang, S. Jung, J.M. Vohs, R.J. Gorte, J. Electrochem. Soc. 153 (2006) A2066–A2070.
[89] Y. Huang, K. Ahn, J.M. Vohs, R.J. Gorte, J. Electrochem. Soc. 151 (2004) A1592–A1597.
[90] S.J. Kim, G.M. Choi, Solid State Ionics 262 (2014) 303–306.
[91] K. Eguchi, T. Hatagishi, H. Arai, Solid State Ionics 86 (1996) 1245–1249.
[92] H. Li, X. Chen, S. Chen, Y. Wu, K. Xie, Int. J. Hydrogen Energy 40 (2015) 7920–7931.
[93] S. Li, R. Yan, G. Wu, K. Xie, J. Cheng, Int. J. Hydrogen Energy 38 (2013) 14943–14951.
[94] J. Li, C. Zhong, X. Meng, H. Wu, H. Nie, Z. Zhan, S. Wang, Fuel Cells. 14 (2014) 1046–1049.
[95] Q. Liu, C. Yang, X. Dong, F. Chen, Int. J. Hydrogen Energy 35 (2010) 10039–10044.
[96] Y. Wang, T. Liu, S. Fang, F. Chen, J. Power Sources 305 (2016) 240–248.
[97] S.J. Kim, K.J. Kim, A.M. Dayaghi, G.M. Choi, Int. J. Hydrogen Energy 41 (2016) 14498–14506.
[98] T. Ogier, F. Mauvy, J.-M. Bassat, J. Laurencin, J. Mougin, J.-C. Grenier, Int. J. Hydrogen Energy 40 (2015) 15885–15892.
[99] J.G. Railsback, Z. Gao, S.A. Barnett, Solid State Ionics 274 (2015) 134–139.
[100] F. Chauveau, J. Mougin, J.M. Bassat, F. Mauvy, J.C. Grenier, J. Power Sources 195 (2010) 744–749.